ISSN (Online) 2393-8021
ISSN (Print) 2394-1588

International Advanced Research Journal in Science, Engineering and Technology
Vol. 2, Issue 5, May 2015

Buckling of laminated composite plates using mesh-less method and trigonometricshear deformation theory

Jeeoot Singh

Department of Mechanical Engineering, Birla Institute of Technology Mesra, Ranchi, India

Abstract: The buckling analysis of single layered orthotropic and cross ply laminated composite plate using trigonometric higher order shear deformation theory and meshless method based on the finite point formulation using multiquadric radial basis function is presented. The convergence of the present method is studied for laminated plates with different shape parameters. After the proper convergence of present method several numerical examples of plates subjected to uniaxial and biaxial loading are under taken. The effect of an anisotropy ratio of material on critical buckling load of the plates is also reported with proper validation of present results with earlier published literature.

Keywords: Composite plate, trigonometric theory, buckling, meshless method.

I. INTRODUCTION

Laminated composite structures are used in many engineering applications such as aerospace, automotive, submarines, sports etc. The mathematical modeling of composite plates is an open discussion. The first order shear deformation proposed by Mindlin [1] and Reissner [2] considers the uniform transverse shear strain and stress over the plate thickness as compared to actual parabolic variation of transverse stress and strain, due to which it under predicts deflection, natural frequency and buckling loads. This theory suits well for thin plates, and can be applied to thick plates adding some stress correction factor. The higher order theory proposed by Reddy [3] is based on five unknowns of first order shear deformation theory but counts parabolic variation of transverse shear stress and strain, hence requirement of stress correction factor is eliminated.

The researchers have employed several analytical and numerical techniques for solving partial differential equations of laminated plates and shells. In the past few years the meshless methods are being used by for the analysis of laminated composite structures. There are the many kind of mesh less methods like element free Galerkin method, meshless local Patrov-Galerkin etc. Radial basis function was applied by Xiang et al [4,5] for linear flexural and free vibration analysis of the laminated composite and sandwich plates. Castro et al [6] used wavelet collocations for static analysis of sandwich plates using layer wise theory. In the recent years Ferreira et al [7,8] used wavelets and Wendland radial basis function for buckling analysis of laminated composite plates. Liew and Huang [9] used moving least-squares differential quadrature for bending and buckling; Liew et al [10,11] used reproducing kernel approximations and meshfree method for buckling analysis of isotropic circular and skew plates. In the present paper multiquadrics radial basis function is used for buckling analysis of laminated composite and orthotropic plates subjected to uniaxial and biaxial loading.

II. MULTIQUADRIC RADIAL BASIS FUNCTION METHOD

Radial basis function based formulation works on the principle of interpolation of scattered data over entire domain. Consider a two dimensional domain having N_B

DOI 10.17148/IARJSET.2015.2504

ISSN (Online) 2393-8021
ISSN (Print) 2394-1588
International Advanced Research Journal in Science, Engineering and Technology
Vol. 2, Issue 5, May 2015

boundary nodes and N_D interior nodes. The variable u over the domain and boundary is interpolated in the form of radial basis function. Most commonly used radial basis functions are:

$g = r^{2c}\log r$	Logarithmic or thin plate spline
$g = e^{-c^2 \times r}$	Gaussian function
$g = r^c$	c=1,2,3,4… Polynomial function
$g = \left(r^2 + c^2\right)^{1/2}$	Multiquadrics function
$g = \left(r^2 + c^2\right)^{-1/2}$	Inverse multiquadrics function

Where, $r = \left\| X - X_j \right\| = \sqrt{\left(x - x_j\right)^2 + \left(y - y_j\right)^2}$

The radial basis functions solve the partial differential equations considering a scattered data over the domain. In the present work multiquadrics radial basis function is used. The solution of the any differential equations is assumed in terms of radial basis function as;

$$u = \sum_{j=1}^{N} \alpha_j^u g\left(\left\| X - X_j \right\|, c\right) \quad \textbf{(1.1)}$$

Where, N is total numbers of nodes which is equal to summation of boundary nodes N_B and domain interior nodes N_D. $g\left(\left\| X - X_j \right\|, c\right)$ is radial basis function, α_j^u is unknown coefficient. $\left\| X - X_j \right\|$ is the radial distance between two nodes.

The given partial differential is expressed and boundary and interior nodes

$Lu(X) = \lambda u(X)$, Interior nodes (i = 1: N_D)

$Bu(X) = 0$, Boundary nodes (i = N_D + 1: N_B)

In matrix form above equations are expressed as:

$$\begin{bmatrix} Lu \\ Bu \end{bmatrix} \{X\} = \lambda \begin{bmatrix} u \\ 0 \end{bmatrix} \{X\} \quad \textbf{(1.2)}$$

Where X is eigenvectors, L and B are the differential operator, u is the variable which is replaced by radial basis function. λ is eigenvalue and obtained by standard Eigen solvers of computational software.

III. GOVERNING DIFFERENTIAL EQUATIONS AND ITS DISCRETIZATION

A square plate having edge length a along x and y direction, thickness h along z direction made up of perfectly bonded laminas and subjected to in plane load N_{xb} N_{yb} and N_{xyb} is considered and mathematical formulation of the actual physical problem of the laminated composite plate subjected to mechanical loading is presented. The displacement field at any point in the laminated composite plate made up of perfectly bonded laminas of uniform thickness is expressed as:

$$u'(x,y,z) = u(x,y) - z\frac{\partial w}{\partial x} + f(z)\phi_x$$

$$v'(x,y,z) = v(x,y) - z\frac{\partial w}{\partial y} + f(z)\phi_y$$

$$w'(x,y) = w(x,y) \quad \textbf{(2)}$$

Where, $f(z) = \frac{h}{\pi}\sin\left(\frac{\pi z}{h}\right)$ is transverse shear stress function proposed by Tauratier [12] and the parameters u', v' and w' are the in-plane and transverse displacements of the plate at any point (x, y, z) in x, y and z directions, respectively.

u, v and w are the displacements at mid plane of the plate at any point (x, y) in x, y and z directions, respectively.

The functions ϕ_x and ϕ_y are the higher order rotations of the normal to the mid plane due to shear deformation about y and x axes, respectively.

Combining the linear strain-displacement relations with assumed displacement field and using variational approach, the descretised GDEs of the plate are obtained and expressed as:

ISSN (Online) 2393-8021
ISSN (Print) 2394-1588

International Advanced Research Journal in Science, Engineering and Technology
Vol. 2, Issue 5, May 2015

$$\sum_{j=1}^{N}\alpha_j^{u}\left(A_{11}\frac{\partial^2 g}{\partial x^2}+A_{66}\frac{\partial^2 g}{\partial y^2}+2A_{16}\frac{\partial^2 g}{\partial x\partial y}\right)+\sum_{j=1}^{N}\alpha_j^{v}\left(A_{12}\frac{\partial^2 g}{\partial x\partial y}+A_{16}\frac{\partial^2 g}{\partial x^2}+A_{66}\frac{\partial^2 g}{\partial x\partial y}+A_{26}\frac{\partial^2 g}{\partial y^2}\right)$$
$$+\sum_{j=1}^{N}\alpha_j^{w}\left(-B_{11}\frac{\partial^3 g}{\partial x^3}-B_{12}\frac{\partial^3 g}{\partial x\partial y^2}-2B_{16}\frac{\partial^3 g}{\partial y\partial x^2}-B_{16}\frac{\partial^3 g}{\partial y\partial x^2}-2B_{66}\frac{\partial^3 g}{\partial x\partial y^2}-B_{26}\frac{\partial^3 g}{\partial y^3}\right)+$$
$$\sum_{j=1}^{N}\alpha_j^{\varphi_y}\left(E_{12}\frac{\partial^2 g}{\partial x\partial y}+E_{16}\frac{\partial^2 g}{\partial x^2}+E_{22}\frac{\partial^2 g}{\partial y^2}+E_{66}\frac{\partial^2 g}{\partial x\partial y}\right)+\sum_{j=1}^{N}\alpha_j^{\varphi_x}\left(E_{11}\frac{\partial^2 g}{\partial x^2}+2E_{16}\frac{\partial^2 g}{\partial x\partial y}+E_{66}\frac{\partial^2 g}{\partial y^2}\right)=0$$

(3.1)

$$\sum_{j=1}^{N}\alpha_j^{u}\left(A_{16}\frac{\partial^2 g}{\partial x^2}+A_{66}\frac{\partial^2 g}{\partial x\partial y}+A_{12}\frac{\partial^2 g}{\partial x\partial y}+A_{26}\frac{\partial^2 g}{\partial y^2}\right)+\sum_{j=1}^{N}\alpha_j^{v}\left(2A_{26}\frac{\partial^2 g}{\partial x\partial y}+A_{66}\frac{\partial^2 g}{\partial x^2}+A_{22}\frac{\partial^2 g}{\partial y^2}\right)$$
$$+\sum_{j=1}^{N}\alpha_j^{w}\left(-B_{16}\frac{\partial^3 g}{\partial x^3}-B_{26}\frac{\partial^3 g}{\partial x\partial y^2}-2B_{26}\frac{\partial^3 g}{\partial x\partial y^2}-2B_{66}\frac{\partial^3 g}{\partial x^2\partial y}-B_{12}\frac{\partial^3 g}{\partial x^2\partial y}-B_{22}\frac{\partial^3 g}{\partial y^3}\right)+$$
$$\sum_{j=1}^{N}\alpha_j^{\varphi_x}\left(E_{16}\frac{\partial^2 g}{\partial x^2}+E_{66}\frac{\partial^2 g}{\partial x\partial y}+E_{12}\frac{\partial^2 g}{\partial x\partial y}+E_{26}\frac{\partial^2 g}{\partial y^2}\right)+\sum_{j=1}^{N}\alpha_j^{\varphi_y}\left(2E_{26}\frac{\partial^2 g}{\partial x\partial y}+E_{66}\frac{\partial^2 g}{\partial x^2}+E_{22}\frac{\partial^2 g}{\partial y^2}\right)=0$$

(3.2)

$$\sum_{i=1}^{N}\alpha_j^{u}\left(B_{11}\frac{\partial^3 u}{\partial x^3}+3B_{16}\frac{\partial^3 u}{\partial x^2\partial y}+\left(B_{12}+2B_{66}\right)\frac{\partial^3 u}{\partial x\partial y^2}+B_{26}\frac{\partial^3 u}{\partial y^3}\right)+$$
$$\sum_{i=1}^{N}\alpha_j^{v}\left(B_{22}\frac{\partial^3 v}{\partial y^3}+3B_{26}\frac{\partial^3 v}{\partial x\partial y^2}+\left(B_{12}+2B_{66}\right)\frac{\partial^3 v}{\partial x^2\partial y}+B_{16}\frac{\partial^3 v}{\partial x^3}\right)-$$
$$\sum_{i=1}^{N}\alpha_j^{w}\left(D_{11}\frac{\partial^4 w}{\partial x^4}+\left(2D_{12}+4D_{66}\right)\frac{\partial^4 w}{\partial x^2\partial y^2}+4D_{16}\frac{\partial^4 w}{\partial x^3\partial y}+4D_{26}\frac{\partial^4 w}{\partial x\partial y^3}+D_{22}\frac{\partial^4 w}{\partial y^4}\right)+$$
$$\sum_{i=1}^{N}\alpha_j^{\varphi_x}\left(F_{11}\frac{\partial^3 \varphi_x}{\partial x^3}+3F_{16}\frac{\partial^3 \varphi_x}{\partial x^2\partial y}+\left(F_{12}+2F_{66}\right)\frac{\partial^3 \varphi_x}{\partial x\partial y^2}+F_{26}\frac{\partial^3 \varphi_x}{\partial y^3}\right)+$$
$$\sum_{i=1}^{N}\alpha_j^{\varphi_y}\left(+F_{22}\frac{\partial^3 \varphi_y}{\partial y^3}+3F_{26}\frac{\partial^3 \varphi_y}{\partial x\partial y^2}+\left(F_{12}+2F_{66}\right)\frac{\partial^3 \varphi_y}{\partial x^2\partial y}+F_{16}\frac{\partial^3 \varphi_y}{\partial x^3}\right)=$$
$$N_{xb}\frac{\partial^2 w}{\partial x^2}+N_{yb}\frac{\partial^2 w}{\partial y^2}+2N_{xyb}\frac{\partial^2 w}{\partial x\partial y}$$

(3.3)

$$\sum_{j=1}^{N}\alpha_j^{u}\left(E_{11}\frac{\partial^2 g}{\partial x^2}+2E_{16}\frac{\partial^2 g}{\partial x\partial y}+E_{66}\frac{\partial^2 g}{\partial y^2}\right)+\sum_{j=1}^{N}\alpha_j^{v}\left(E_{12}\frac{\partial^2 g}{\partial x\partial y}+E_{16}\frac{\partial^2 g}{\partial x^2}+E_{26}\frac{\partial^2 g}{\partial y^2}E_{66}\frac{\partial^2 g}{\partial x\partial y}\right)$$
$$+\sum_{j=1}^{N}\alpha_j^{w}\left(-F_{11}\frac{\partial^3 g}{\partial x^3}-F_{12}\frac{\partial^3 g}{\partial x\partial y^2}-3F_{16}\frac{\partial^3 g}{\partial y\partial x^2}-F_{26}\frac{\partial^3 g}{\partial y^3}-2F_{66}\frac{\partial^3 g}{\partial x\partial y^2}\right)+$$
$$\sum_{j=1}^{N}\alpha_j^{\varphi_x}\left(H_{11}\frac{\partial^2 g}{\partial x^2}+2H_{16}\frac{\partial^2 g}{\partial x\partial y}+H_{66}\frac{\partial^2 g}{\partial y^2}-A_{55}g\right)+$$
$$\sum_{j=1}^{N}\alpha_j^{\varphi_y}\left(H_{12}\frac{\partial^2 g}{\partial x\partial y}+H_{16}\frac{\partial^2 g}{\partial x^2}+H_{22}\frac{\partial^2 g}{\partial y^2}+H_{66}\frac{\partial^2 g}{\partial x\partial y}-A_{45}g\right)=0$$

(3.4)

$$\sum_{j=1}^{N}\alpha_j^{u}\left(E_{16}\frac{\partial^2 g}{\partial x^2}+E_{66}\frac{\partial^2 g}{\partial x\partial y}+E_{12}\frac{\partial^2 g}{\partial x\partial y}+E_{26}\frac{\partial^2 g}{\partial y^2}\right)+\sum_{j=1}^{N}\alpha_j^{v}\left(2E_{26}\frac{\partial^2 g}{\partial x\partial y}+E_{66}\frac{\partial^2 g}{\partial x^2}+E_{22}\frac{\partial^2 g}{\partial y^2}\right)+$$
$$\sum_{j=1}^{N}\alpha_j^{w}\left(-F_{16}\frac{\partial^3 g}{\partial x^3}-2F_{66}\frac{\partial^3 g}{\partial y\partial x^2}-3F_{26}\frac{\partial^3 g}{\partial x\partial y^2}-F_{12}\frac{\partial^3 g}{\partial y\partial x^2}-F_{22}\frac{\partial^3 g}{\partial y^3}\right)+$$
$$\sum_{j=1}^{N}\alpha_j^{\phi_x}\left(H_{16}\frac{\partial^2 g}{\partial x^2}+H_{66}\frac{\partial^2 g}{\partial x\partial y}+H_{12}\frac{\partial^2 g}{\partial x\partial y}+H_{26}\frac{\partial^2 g}{\partial y^2}-A_{45}g\right)+$$
$$\sum_{j=1}^{N}\alpha_j^{\phi_y}\left(2H_{26}\frac{\partial^2 g}{\partial x\partial y}+H_{66}\frac{\partial^2 g}{\partial x^2}+H_{22}\frac{\partial^2 g}{\partial y^2}-A_{44}g\right)=0$$

(3.5)

The boundary conditions for a simply supported edge are:

$$x=0,a: v=0:\phi_y=0; w=0: M_x=0: N_x=0$$
$$y=0,b: u=0:\phi_x=0: w=0: M_y=0: N_y=0$$

IV. EIGEN VALUE BUCKLING ANALYSIS

The discretized governing differential equation for the plate subjected to inplane loads is expressed as eigen value for predicting the critical buckling load

$$\left[K_E\right]-N_{cr}\left[K_G\right]\times\{\delta\}=\{0\}$$

Where K_E is the stiffness matrix and K_G is geometric stiffness matrix, N_{cr} is eigen value or critical buckling load

V. RESULTS AND DISCUSSION

The several numerical examples are solved for demonstration of accuracy of the present method. In the present work three and four layered cross ply laminated and single layered orthotropic plate subjected to uniaxial and biaxial compression are undertaken.

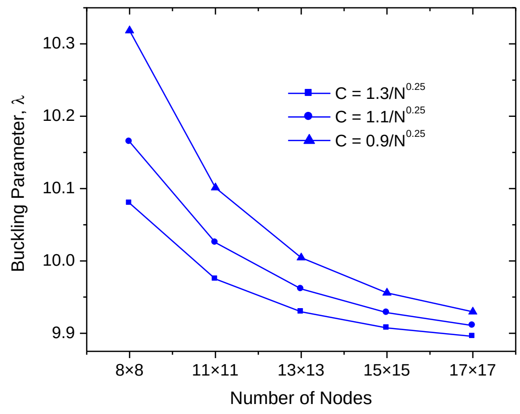

Figure 1: Convergence of present method for cross ply plate with different values of shape parameters (E1/E2 = 10)

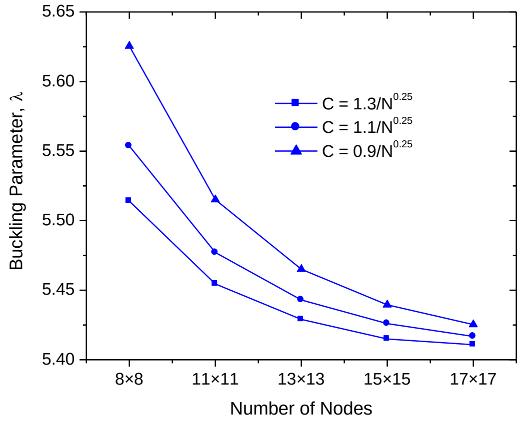

Figure 2: Convergence of present method for cross ply plate with different values of shape parameters (E1/E2 = 3)

ISSN (Online) 2393-8021
ISSN (Print) 2394-1588

International Advanced Research Journal in Science, Engineering and Technology
Vol. 2, Issue 5, May 2015

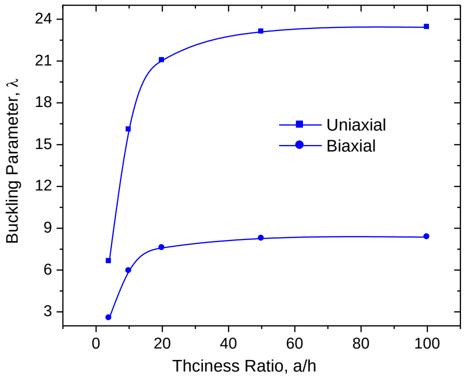

Figure 3: Effect of width to thickness ratio on critical buckling load of orthotropic plate subjected to uniaxial and biaxial loading

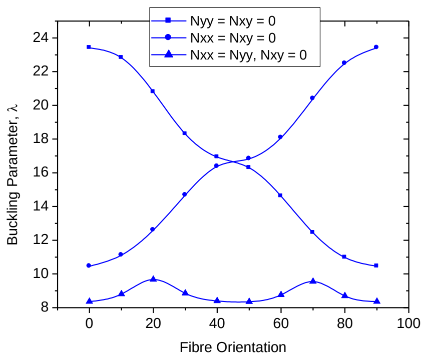

Figure 4: Effect of fibre orientation on critical buckling load of orthotropic plate subjected to uniaxial and biaxial loading

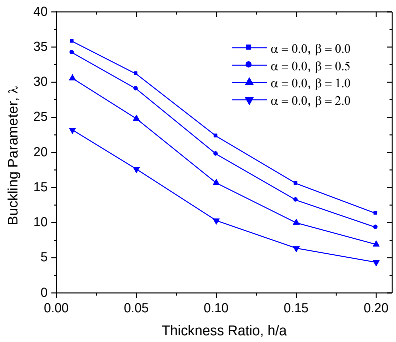

Figure 5: Effect of inplane shear on buckling load of simply supported symmetric cross ply plate subjected to uniaxial compression

Table 1: Convergence studies of present method for critical buckling load of (0/90/0) cross ply plate subjected to uniaxial edge compression (a/h = 10)

c	Method	Orthotropic Ratio (E_1/E_2)				
		3	10	20	30	40
1.3/$N^{0.25}$	[7]	5.3869	9.86010	14.9746	19.0175	22.3070
	[13]	5.3933	9.94060	15.2980	19.6740	23.3400
	(11×11)	5.4545	9.97500	15.1443	19.2416	22.5908
	(13×13)	5.4290	9.92970	15.0796	19.1685	22.5201
	(15×15)	5.4149	9.90740	15.0485	19.1367	22.4953
	(17×17)	5.4108	9.89560	15.0326	19.1227	22.4881
1.1/$N^{0.25}$	[7]	5.3869	9.86010	14.9746	19.0175	22.3070
	[13]	5.3933	9.94060	15.2980	19.6740	23.3400
	(11×11)	5.4771	10.0254	15.2169	19.3117	22.6343
	(13×13)	5.4430	9.96130	15.1226	19.2054	22.5321
	(15×15)	5.4260	9.92850	15.0777	19.1616	22.5012
	(17×17)	5.4168	9.91060	15.0326	19.1436	22.4962
0.9/$N^{0.25}$	[7]	5.3869	9.86010	14.9746	19.0175	22.3070
	[13]	5.3933	9.94060	15.2980	19.6740	23.3400
	(11×11)	5.5151	10.1012	15.3144	19.3822	22.6089
	(13×13)	5.4651	10.0044	15.1711	19.2156	22.4417
	(15×15)	5.4395	9.95590	15.1052	19.1513	22.4017
	(17×17)	5.4253	9.92970	15.0733	19.1297	22.4100

ISSN (Online) 2393-8021
ISSN (Print) 2394-1588
International Advanced Research Journal in Science, Engineering and Technology
Vol. 2, Issue 5, May 2015

Table 2: Effect of width to thickness ratio of an orthotropic plate on critical buckling load subjected to uniaxial and biaxial compression

a/h	Loading	Present	Sundaresan [14]	Reddy [15]
4	Uniaxial	6.61550	--	-------
	Biaxial	2.54870	--	--
10	Uniaxial	16.0657	15.8740	15.874
	Biaxial	5.93700	5.83720	5.8370
20	Uniaxial	21.0418	--	20.953
	Biaxial	7.59140	--	7.5550
50	Uniaxial	23.0906	--	--
	Biaxial	8.25900	--	--
100	Uniaxial	23.4159	23.3817	23.381
	Biaxial	8.36220	8.36980	8.3690

Table 3: Effect of anisotropic ratio on critical buckling load for symmetric cross ply plate subjected to uniaxial edge compression (a/h = 10)

Laminate	Orthotropic Ratio (E_1/E_2)				
	3	10	20	30	40
0/90/0	5.4108	9.8956	15.0326	19.1227	22.4881
0/90/90/0	5.4161	10.025	15.5252	20.0520	23.8166

Table 4: Effect of anisotropic ratio on critical buckling load for symmetric cross ply plate subjected to biaxial edge compression (a/h = 10)

Laminate	Orthotropic Ratio (E_1/E_2)				
	3	10	20	30	40
0/90/0	2.7056	4.9493	7.5220	8.9756	10.1973
0/90/90/0	2.7083	5.0455	7.7929	10.0498	11.9452

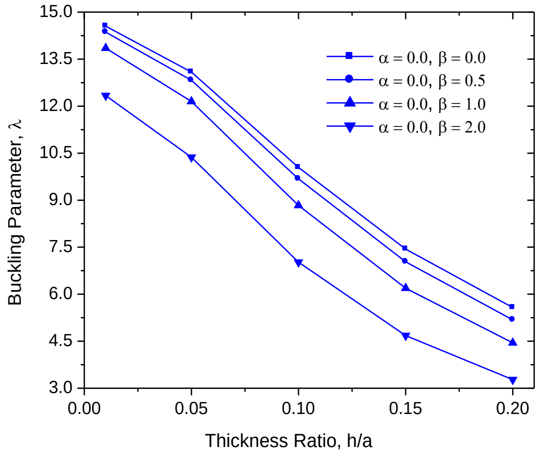

Figure 6: Effect of inplane shear on buckling load of simply supported symmetric cross ply plate subjected to biaxial compression

Convergence study:

The square cross ply (0/90/0) moderately thick laminate composite plate subjected to uniaxial compression with simply supported edges is considered for convergence of the present method. The convergence is investigated for different values of shape parameters. The relative material properties of an orthotropic lamina are taken as

$E_1/E_2 = 3, 10, 20, 30, 40$; $G_{12} = G_{13} = 0.6E_2$; $G_{23} = 0.5E_2$; $\nu = 0.25$

It is found that the present method is fast converging for greater value of shape parameters. The convergence is achieved for 17×17 domain nodes. The present multiquadrics results are compared with earlier published results by Reddy and Phan [13] and wavelets results of Ferreira et al [7]. It is observed that the present method produces the results with good accuracy and shown in Table 1 for different value of shape parameters and anisotropy ratio (E_1/E_2). **Figures 1 and 2** shows convergence of present method with different values of shape parameter and orthotropy ratio E_1/E_2 of 10 and 3 respectively. The results are presented in non dimensional form using expression:

$$\lambda_{N_{cr}} = \frac{N_{cr} a^2}{E_2 h^3}$$

 DOI 10.17148/IARJSET.2015.2504

ISSN (Online) 2393-8021
ISSN (Print) 2394-1588

International Advanced Research Journal in Science, Engineering and Technology
Vol. 2, Issue 5, May 2015

Orthotropic plate:

In this section square orthotropic plate having different values of length to thickness ratio subjected to uniaxial and biaxial compression with simply supported edges is considered. The relative material properties of an orthotropic lamina are taken as

$E_1/E_2 = 25$; $G_{12} = G_{13} = 0.5E_2$; $G_{23} = 0.2E_2$; $\nu = 0.25$

Table 2 shows the critical buckling load factor for orthotropic plate subjected to uniaxial and biaxial loading. The present results are compared with earlier results of **Reddy [15];** Sundaresan et al [14] and found accurate. The **Figure 3 and 4** shows the effect of width to thickness ratio and fibre orientation on the critical buckling load factor of the plate as expected.

Cross ply laminated composite plate:

The three and four layered symmetric cross ply plates with simply supported edge subjected to uniaxial and biaxial compression is considered. The relative material properties of an orthotropic lamina are taken as

$E_1/E_2 = 3, 10, 20, 30, 40$; $G_{12} = G_{13} = 0.6E_2$; $G_{23} = 0.5E_2$; $\nu = 0.25$

Table 3 shows the critical buckling load factor for [0/90/0] and [0/90/90/0] cross ply moderately thick plates (a/h=10) subjected to uniaxial loading with different values of anisotropy ratio. It is observed that the present meshless method proved good accuracy for buckling analysis.

Table 4 shows the critical buckling load factor of symmetric cross ply moderately thick plate subjected to biaxial loading with different values of anisotropy ratio.

Figure 5 and 6 shows the effect on inplane shear load on the buckling parameter for cross ply plate subjected to uniaxial and biaxial loading for the material having orthotropic ratio E_1/E_2 of 40. The effect has been studied over the wide range of span to thickness ratio. It is observed that when value of inplane shear load is small say $N_{xy}/N_x = 0.5$ the effect on buckling parameter is observed to be negligible, where as when $N_{xy}/N_x = 2$ the buckling load factor is highly reduced. Further, the effect of in plane shear is more for thick plates as compare to thin plates.

VI. CONCLUSION

The buckling analysis of laminated composite and orthotropic plates using radial basis functions is presents. Both uniaxial and biaxial loading of the plates are under taken. The present results are compared several earlier published literature. The plate kinematics is based on the trigonometric shear deformation theory and eigen problem is defined in terms of radial basis function to compute the critical buckling loads. The present shows good accuracy and convergence for the plate problems. This method can be used as a new tool for the plate buckling analysis.

REFERENCES

[1]. Mindlin RD. Influence of rotary inertia and shear on flexural motions of isotropic elastic plates. ASME Journal of Applied Mechanics 18 (1951) 31–38.
[2]. Reissner E. Reflection on the theory of elastic plates. ASME Journal of Applied Mechanics 38 (1945) 1453–1464.
[3]. Reddy JN. A simple higher-order theory for laminated composite plates. ASME Journal of Applied Mechanics 51 (1984) 745-752
[4]. Xiang S, Ke-ming Wang, Yan-ting Ai, Yun-dong Sha, Shi H. Analysis of isotropic, sandwich and laminated plates by a meshless method and various shear deformation theories. Composite Structures 91(2009) 31-37.
[5]. Xiang S, Shao-xi Jiang, Ze-yang Bi, Yao-xing Jin, Ming-sui Yang. A nth-order meshless generalization of Reddy's third-order shear deformation theory for the free vibration on laminated composite plates. Composite Structures 93 (2011) 299–307
[6]. Castro LMS, Ferreira AJM, Bertoluzza S, Batra RC, Reddy JN. A wavelet collocation method for the static analysis of sandwich plates using a layerwise theory. Composite Structures 92 (2010) 1786–179
[7]. Ferreira AJM, Castro LM, Roque CMC, Reddy JN, Bertoluzza S. Buckling analysis of laminated plates by wavelets. Computers and Structures 89 (2011) 626–630
[8]. Ferreira AJM, Roque CMC, Neves AMA, Jorge RMN, Soares CMM, Liew KM. Buckling and vibration analysis of isotropic and laminated plates by radial basis functions. Composites: Part B Engineering (2010)
[9]. Liew KM, Huang YQ. Bending and buckling of thick symmetric rectangular laminates using the moving least-squares differential quadrature method. International Journal of Mechanical Sciences 45 (2003) 95–114
[10]. Liew KM, Chen XL, Reddy JN. Meshfree radial basis function method for buckling analysis of non-uniformly loaded arbitrarily shaped shear deformable plates. Computer Methods in Applied Mechanics Engineering 193 (2004a) 205–224
[11]. Liew KM, Wang J, Ng TY, Tan MJ. Free vibration and buckling analyses of shear-deformable plates based on FSDT meshfree method Journal of Sound and Vibration 276 (2004b) 997–1017
[12]. Touratier M. An efficient standard plate theory. International Journal Engineering Science 29 (1991) 901–916.
[13]. Reddy JN, Phan ND. Stability and vibration of isotropic, orthotropic and laminated plates according to a higher-order shear deformation theory. Journal of Sound and Vibrations 98 (1985)157–170.
[14]. Sundaresan P, Singh G, Rao GV. Buckling of moderately thick rectangular composite plates subjected to partial edge compression. International Journal of Mechanical Sciences 40 (1998) 1105-1117
[15]. Reddy JN. Mechanics of Laminated Composite Plates and Shells. CRC Press. 2004